INTERNATIONAL JOURNAL OF CLIMATOLOGY
Int. J. Climatol. **24**: 1973–1982 (2004)
Published online 7 October 2004 in Wiley InterScience (www.interscience.wiley.com). DOI: 10.1002/joc.1090

SHORT COMMUNICATION

THE NEAR-SURFACE WIND FIELD OVER THE ANTARCTIC CONTINENT

N. P. M. VAN LIPZIG,[a,*] J. TURNER,[a] S. R. COLWELL[a] and M. R. VAN DEN BROEKE[b]
[a] *British Antarctic Survey, Cambridge, UK*
[b] *Institute for Marine and Atmospheric Research, Utrecht, The Netherlands*

Received 28 November 2003
Revised 2 July 2004
Accepted 2 July 2004

ABSTRACT

A 14 year integration with a regional atmospheric model has been used to determine the near-surface climatological wind field over the Antarctic ice sheet at a horizontal grid spacing of 55 km. Previous maps of the near-surface wind field were generally based on models ignoring the large-scale pressure-gradient forcing term in the momentum equation. Presently, state-of-the-art atmospheric models include all pressure-gradient forcing terms. Evaluation of our model output against *in situ* data shows that the model is able to represent realistically the observed increase in wind speed going from the interior to the coast, as well as the observed wind direction at South Pole and Dumont d'Urville and the bimodal wind distribution at Halley. Copyright © 2004 Royal Meteorological Society.

KEY WORDS: wind field; Antarctica; atmospheric modelling

1. INTRODUCTION

The near-surface wind field is an important meteorological element over the Antarctic continent. The strong and persistent flow in the coastal region affects the redistribution of snow. On a local scale, the transport of snow by the wind is an important term in the surface mass balance (defined as the sum of precipitation, sublimation, snow transport by the wind and run-off). On the scale of the entire Antarctic ice sheet, it is estimated that about 10% of the total net input of snow is removed by transport of snow into the sea (Giovinetto *et al*., 1992). In addition, the near-surface winds affect the sublimation of blowing snow, another term affecting the surface mass balance of the Antarctic ice sheet (e.g. Bintanja, 2001). Furthermore, extreme wind conditions restrict field operations, and the time-varying wind field determines transport of biological and chemical particles. Katabatic winds are partly responsible for the development of a pronounced circumpolar vortex in the middle and upper troposphere and they are, therefore, essential in prescribing large-scale circulations (Parish and Bromwich, 1987). It is clear that, for a range of studies, detailed information on the near-surface wind field is needed.

In situ data, remote sensing observations and modelling techniques have been used to study the flow near the surface of the Antarctic ice sheet (Ball, 1960; D'Aguanno, 1986; Parish and Waight, 1987; Bromwich, 1989; Gallée and Schayes, 1992; Heinemann, 1997). Mather and Miller (1967) used the available observations from the stations and data on sastrugi orientation to produce an Antarctic-wide map of surface stream lines. This provided the first broad-scale indication of the wind directions, but did not provide detailed information on the wind speeds.

* Correspondence to: N. P. M. van Lipzig, Meteorologisches Institut, Universität München, Theresienstr. 37, 80333 München, Germany ; e-mail: nicole@meteo.physik.uni-muenchen.de

Numerical models offer a powerful means of investigating the wind field. The elegant one-layer model of Ball (1960) has been used in a number of studies, and in particular has been applied by Parish and Bromwich (1987) to generate an improved stream-line map for the Antarctic. Later, Parish and Bromwich (1991) used an early primitive equation three-dimensional model to study Antarctic surface winds. In these studies the large-scale pressure-gradient forcing (LSC) is not taken into account. This term, however, is important for calculating the near-surface wind field (Parish and Cassano, 2001; van den Broeke *et al*., 2002).

Presently, most state-of-the-art models that are used to study the climate of Antarctica include LSC. Some of these models operate at high horizontal grid spacing up to about 100 km (e.g. Genthon *et al*., 2002). Even higher horizontal grid spacing can be obtained with regional models, and in various studies they have been used to examine details of the Antarctic wind field (Heinemann, 1997; Bailey *et al*., 2004). However, most of these models only cover parts of the ice sheet or limited time periods (less than 1 year). The goal of this paper is to present a new climatological near-surface wind field for the entire Antarctic ice sheet based on output from the high-resolution Regional Atmospheric Climate Model (RACMO).

The model has been integrated for the period 1980–93 with a horizontal grid spacing of 55 km, which is an improvement compared with most global models and reanalysis projects: for example, the grid spacing of RACMO is about half the value used in the European Centre for Medium-range Weather Forecasts (ECMWF) reanalysis project (ERA-40). The RACMO domain covers the whole of the Antarctic continent and part of the Southern Ocean. The daily variations in sea-surface temperature and sea-ice extent were prescribed from satellite observations.

In this paper, the resultant wind field is compared with the *in situ* data, obtained as part of the Scientific Committee on Antarctic Research READER (Reference Antarctic Data for Environmental Research) project (Turner *et al*., 2004). This new data set of Antarctic climate data, produced by re-deriving mean values from the original synoptic reports, can be found at http://www.antarctica.ac.uk/met/READER/.

2. DESCRIPTION OF THE RACMO

The RACMO uses the physical parameterizations of the ECHAM-4 model (Roeckner *et al*., 1996). In the lateral boundary zone of the model, the temperature, the specific humidity, the zonal and meridional components of the wind, and the surface pressure are relaxed towards ERA-15-data using a technique by Davies (1976). The field that is used in the calculations is a linear combination of the field supplied by ERA-15 and the prognostically calculated field. The weighting is performed as a function of the distance to the outer edge of the model. To avoid spurious precipitation in the relaxation zone, the specific humidity is only linked to the ERA-15 fields when inflow into the model domain occurs (Christensen *et al*., 1996). ERA-15 fields are available every 6 h, and a combination of fields is used for every time step in between.

The model is able to represent realistically surface heat exchange processes at a site in Dronning Maud Land (van Lipzig *et al*., 1999). Note that the regions referred to in the text are shown in Figure 1. For a detailed description of the 14 year integration, which is used to generate the wind field, we refer to van Lipzig *et al*. (2002).

Winds (v) at 3 m height and at 10 m height are calculated from the lowest levels by assuming a log–linear relationship between wind speed and height above the surface (z);

$$v(z) = C_1 \ln \frac{z}{z_0} + C_2(z - z_0) \tag{1}$$

where z_0 is the surface roughness length prescribed in the model, where the wind is assumed to be zero. Values for C_1 and C_2 are calculated from the lowest two model levels at about 7 and 35 m above the surface.

3. THE CLIMATOLOGY OF NEAR-SURFACE WINDS

Figure 2 shows the winter (June–August, JJA) climatology of the 7 m wind vectors and stream lines. The wind field is strongly controlled by the orography. A downslope pressure-gradient force exists (van den

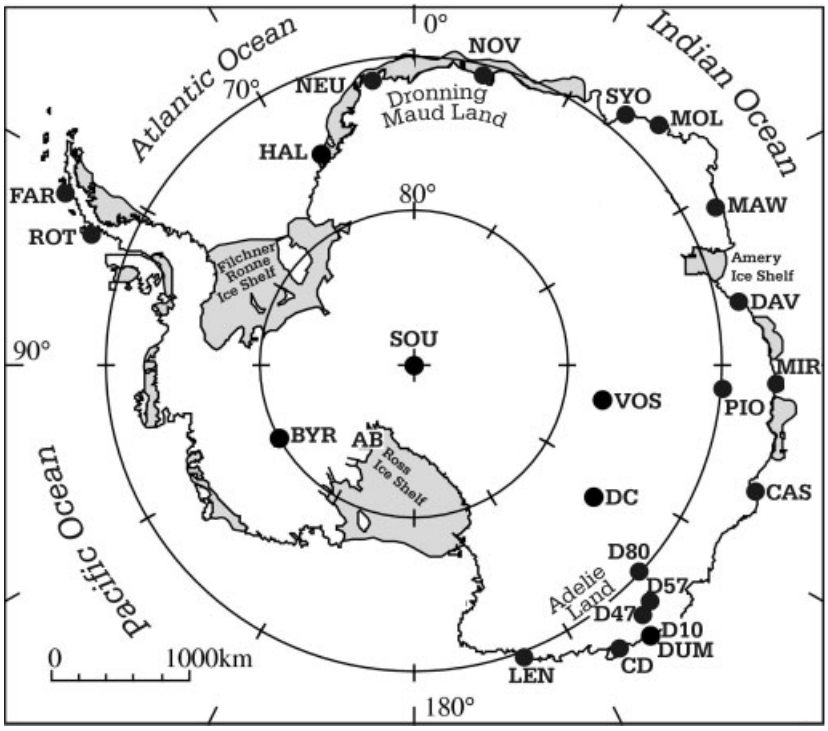

Figure 1. Map with regions and stations mentioned in the text. Abbreviations used: Rothera (ROT), Faraday (FAR), Halley (HAL), Neumayer (NEU), Novolazarevskaya (NOV), Syowa (SYO), Molodezhnaya (MOL), Mawson (MAW), Davies (DAV), Mirny (MIR), Pionerskaya (PIO), Vostok (VOS), Casey (CAS), Dome C (DC), Dumont d'Urville (DUM), Cape Denison (CD), Leningradskaya (LEN), Byrd (BYR), South Pole (SOU), and ice streams A and B (AB; Mercer, van der Veen and Whillans ice stream)

Broeke *et al*., 2002), but the winds are directed away from the fall line by the Coriolis force. The flow is not uniform, but becomes concentrated in confluent patterns at the eastern side of ridges and at the western side of troughs in the surface (Parish and Bromwich, 1987). The maps show many other interesting small-scale features, e.g. a large flow over ice streams A and B, which is the main drainage of air onto the Ross Ice Shelf.

The katabatic forcing (KAT), resulting from a negative deviation of the atmospheric boundary-layer potential temperature from the free-atmosphere potential temperature over sloping terrain, dominates the surface layer momentum budget near the steep coastal slopes. However, for large parts of the Antarctic continent, LSC is the largest term in the momentum equation. For a detailed comparison between the different terms in the momentum equation we refer to van den Broeke and van Lipzig (2003).

Parish and Bromwich (1987) have used sastrugi orientations as a proxy for the near-surface wind direction to evaluate the modelled wind direction. The Parish and Bromwich (1987, 1991) stream-line maps are nearly identical, and correspond both very well to the sastrugi orientation. Parish and Bromwich (1987, 1991) ignored LSC, and KAT is the main pressure gradient forcing term. Because LSC acts in the same direction as KAT, our wind direction is very similar to Parish and Bromwich (1987) and also our stream-line map corresponds closely to the sastrugi orientations. Areas of strong confluence can be identified east of Dumont d'Urville, east of Mirny and west of the Amery Ice Shelf. Both the Parish and Bromwich (1987) map and our map show low wind speeds in the high interior of the East Antarctic ice sheet, higher winds near the coast and a large flow from East to West Antarctica in the region 0–30 °W.

However, there are also differences; e.g. the Parish and Bromwich (1987) map shows southerly winds in coastal West Antarctica, whereas the RACMO winds have a large component directed along the coast. By calculating the RACMO stream lines over the grounded ice sheet and the ice shelves, it is found that the largest confluence zones are not present on the steep slopes; rather, they are found on the flat ice shelves, namely on the western side of the Filchner–Ronne Ice Shelf and on the eastern side of the Ross Ice Shelf.

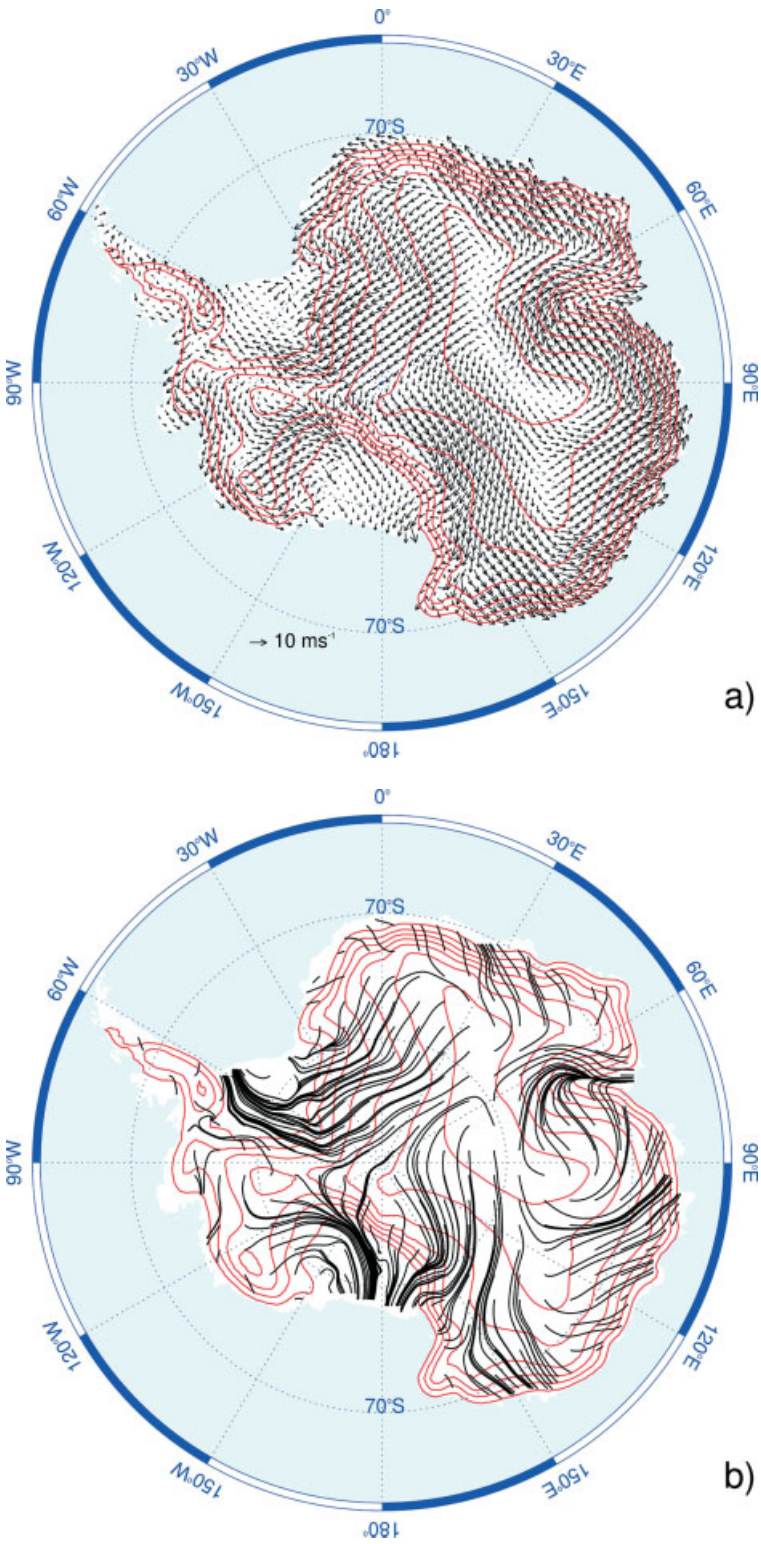

Figure 2. Mean winter (JJA) 7 m wind vector (a) and stream lines (b) for 1980–93. Vectors are shown for every second grid point and stream lines are started every fifth grid point. The elevation of the surface is shown by contour lines in red, which are plotted every 0.5 km

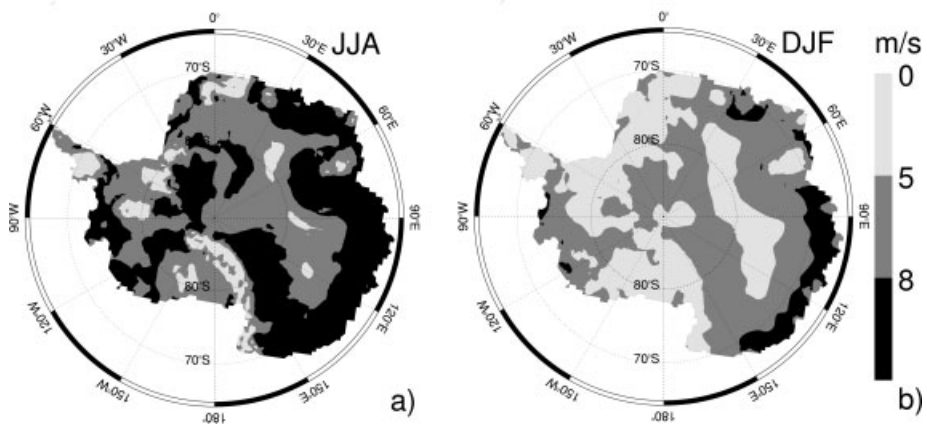

Figure 3. Mean winter (a) and summer (b) 7 m wind speed for 1980–93

In particular, the Filchner–Ronne confluence zone is located in a region where polynias often occur and, therefore, is possibly relevant for studies on air–sea interaction. Note that the regions of strong confluence do not necessarily coincide with regions where the average wind speed is large (Figure 3(a)).

A map derived with ERA-40 data (not shown) shows very similar broad-scale features as Figure 2, indicating that both RACMO and ERA-40 realistically represent the near-surface wind field over Antarctica. The ERA-40 map shows slightly less detail, because the grid spacing in ERA-40 is about twice the value used in RACMO. For example, the outflow of air over ice streams A and B and the outflow from the Amery Ice Shelf are confined to smaller areas in RACMO than in ERA-40.

There is a large seasonal dependency of the wind speed (Figure 3). The average wind speed over the continent is greatest in July (8 m s^{-1}) and least in January (5 m s^{-1}). In summer, KAT is much smaller than in winter and LSC dominates the momentum budget except near the coast, where KAT becomes equally important (van den Broeke *et al*., 2002). The maximum mean winter wind speed of 16.3 m s^{-1} is found at 145.9 °E, 68.9 °S on the western side of the trough in the surface near Cape Denison.

4. EVALUATION OF THE MODEL WINDS

Parish and Bromwich (1991: table I) compared their modelled wind speed and wind directions ϕ with measurements from several stations. For evaluation of RACMO and comparison of our integration with the Parish and Bromwich (1991) integration, we show the measurements given by Parish and Bromwich (1991), the READER data, the Parish and Bromwich (1991) model output and the RACMO output for selected stations in Table I. For RACMO we present the wind speed at the height of the station, namely at 3 m height for the automatic weather stations (AWSs) Byrd, Dome C and Cape Denison and at 10 m height for the manned stations Vostok, Pionerskaya, South Pole and Mirny.

The differences in ϕ between the Parish and Bromwich (1991) measurements and READER are within 10°. The wind speed is greater in READER than in Parish and Bromwich (1991), e.g. at Dome C the difference is 33%. This is probably caused by the fact that the measurements cover different time periods.

The wind direction at the stations is very well represented by both the Parish and Bromwich (1991) model and RACMO, with differences smaller than 10°, except for Mirny, where the zonal component is overestimated in RACMO. The most remarkable difference between RACMO and Parish and Bromwich (1991) is that the RACMO wind speed is 23% lower than the Parish and Bromwich (1991) wind speed. At most stations the agreement with the measurement is much better for RACMO than for Parish and Bromwich (1991), especially at Vostok, Pionerskaya, South Pole, and Mirny. Only at Cape Denison does the Parish and Bromwich (1991) wind speed correspond better to the measurements than the RACMO wind speed.

Table I. Long-term mean wind speed v and wind direction ϕ for stations selected by Parish and Bromwich (1991) (PB91). Measurements selected by Parish and Bromwich (1991) and the READER data are shown together with model winds of Parish and Bromwich (1991) and of RACMO

	Measurements				Model output				
	PB91		READER		PB91		RACMO		
	v (m s^{-1})	ϕ (°)	v (m s^{-1})	ϕ (°)	v (m s^{-1})	ϕ (°)	v-10 m (m s^{-1})	v-3 m (m s^{-1})	ϕ (°)
Byrd	6.4	013	6.9	009	6.6	005		6.9	016
Vostok	4.1	243	5.3	234	8.2	220	6.0		233
Pionerskaya	9.3	131	—	—	14.5	139	9.4		121
South Pole	4.6	039	5.0	041	8.9	045	5.5		052
Dome C	2.0	205	3.0	196	4.4	204		4.2	209
Cape Denison	19.0	161	20.5	162	22.6	157		12.7	156
Mirny	9.7	127	11.3	120	20.8	125	8.8		100

Figure 4 shows the frequency of occurrence of winds in each of 12 direction sectors during the time period 1980–93. Both observations and model output are shown for three stations representing different climatic regimes. South Pole station is located in the interior. Dumont d'Urville is located close to the slopes of Adélie Land, where KAT plays an important role, and the coastal station Halley is located on an ice shelf where katabatics rarely penetrate. The locations of the stations are shown on Figure 1.

For deriving wind directions at South Pole station, the Greenwich meridian is defined north, and 90 °E is defined east. Prevailing winds are from northerly to easterly directions, with high wind-speed cases mainly from the north. This characteristic is represented by all three model grid points surrounding the site where the measurements were performed. Wind roses for the grid points g_0 (closest), g_1 (second closest) and g_2 (third closest) show little variation, indicating that the region around the south polar station is homogeneous. High wind-speed cases are underestimated by the model, which is not surprising given that the model output represents the average over an area of 55×55 km^2.

Dumont d'Urville is located on a small island 1 km north of the coastline of Adélie Land (Pettré *et al.*, 1993). Winds at Dumont d'Urville are most frequently from the south-southeast. Higher wind speeds tend to be correlated with more southerly directions. There is little variation between the sea/sea-ice grid points g_0 and g_2 with east-southeast as the prevailing direction. The land-ice grid point located most closely to Dumont d'Urville is grid point g_1, located on the slopes of Adélie Land at an elevation of 725 m. The wind rose for this grid point corresponds most closely to the wind rose derived from the measurements. For this grid point the prevailing direction is south-southeast, but g_1 experiences more winds from the south than observed at Dumont d'Urville. Interestingly, the prevailing direction at Dumont d'Urville is in between that of the sea/sea-ice grid points and that of the grid point on the slopes of Adélie Land.

At Halley, there is a bimodal wind distribution (Renfrew and Anderson, 2002). Above the boundary layer, at 2 km height, easterly winds are related to the passage of depressions from west to east across the Weddell Sea, whereas westerly winds occur when pressure is high over the Weddell Sea (King, 1989). Interaction between the large-scale pressure-forcing and steep slopes of the ice sheet south of Halley (barrier effects) results in the distribution shown in Figure 4. Owing to the complexity of the region, there are large differences in wind distribution between the selected grid points. The grid point g_0, located most closely to Halley, does not capture the bimodal wind distribution. This grid point is located on the ice shelf, at an elevation of about 30 m, but the model resolution is too coarse to represent this ice shelf as flat terrain, so KAT is not zero. At grid point g_1, located south of Halley at an elevation of 77 m, katabatic winds prevail from east and southeast, as observed in this region (Renfrew and Anderson, 2002). The closest correspondence between model and measurements from Halley is found for grid point g_2, which is a sea-ice grid point located north of the station. This grid point shows the bimodal distribution clearly, but easterlies are shifted anticlockwise, probably due to a weaker barrier effect than at Halley.

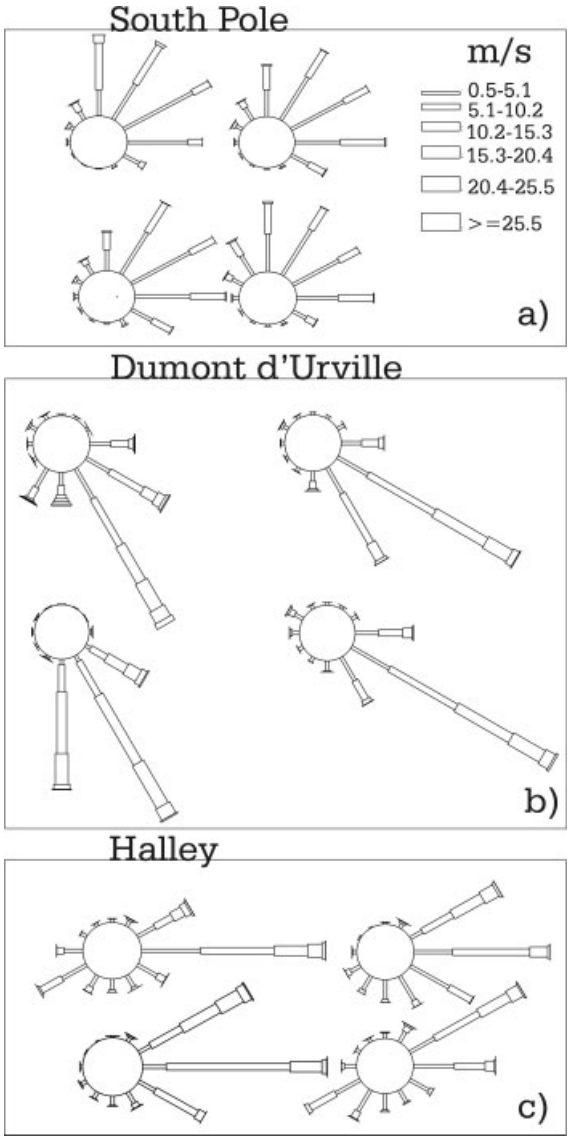

Figure 4. Wind roses for South Pole (a), Dumont d'Urville (b) and Halley (c) calculated from 6 h values over the 14 year period (1980–93). The wind directions are divided into 30° bins and the wind speeds into 10 knot bins from 1 to 40 knots (1 knot = 0.51 m s^{-1}). The panels refer to: observations (upper left), model output at g_0 (upper right), g_1 (lower left), g_2 (lower right), surrounding the site. Grid point g_0 is the point closest to the station. All points are land-ice grid points except Dumont d'Urville g_0 and g_2 and Halley g_2

For Halley, the wind roses are shown separately for the winter months (JJA) and for the summer months (December–February, DJF) in Figure 5. The frequency of occurrence of strong (weak) winds is larger (smaller) in winter than in summer. However, the frequency of occurrence of a specific wind direction remains rather constant throughout the year, which implies that the bimodal distribution at Halley reflects different synoptic regimes rather than the seasonality. These are general features for all sites considered and they are well represented by RACMO.

Figure 6(a) shows the 14 year mean modelled and observed 10 m winds at 15 stations in the READER data set. The difference in wind speed between coastal east Antarctica (Molodezhnaya, Mawson and Dumont d'Urville) and the interior (South Pole and Vostok) is correctly represented by the model. For 11 out of the 15 sites, the model bias is smaller than 1.4 m s^{-1}. The mean absolute bias is 1.6 m s^{-1}.

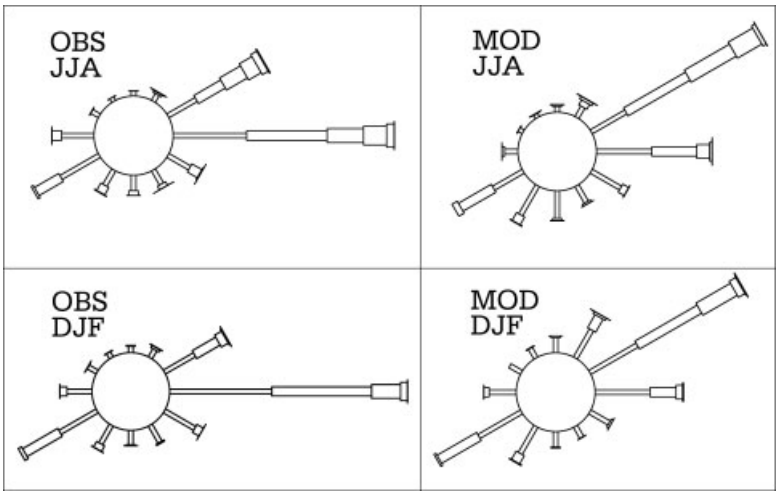

Figure 5. As Figure 4 for Halley, but for winter (JJA) and summer (DJF) separately. Left panels show the wind roses derived from the observations and right panels show the wind roses derived from RACMO model output at g_2

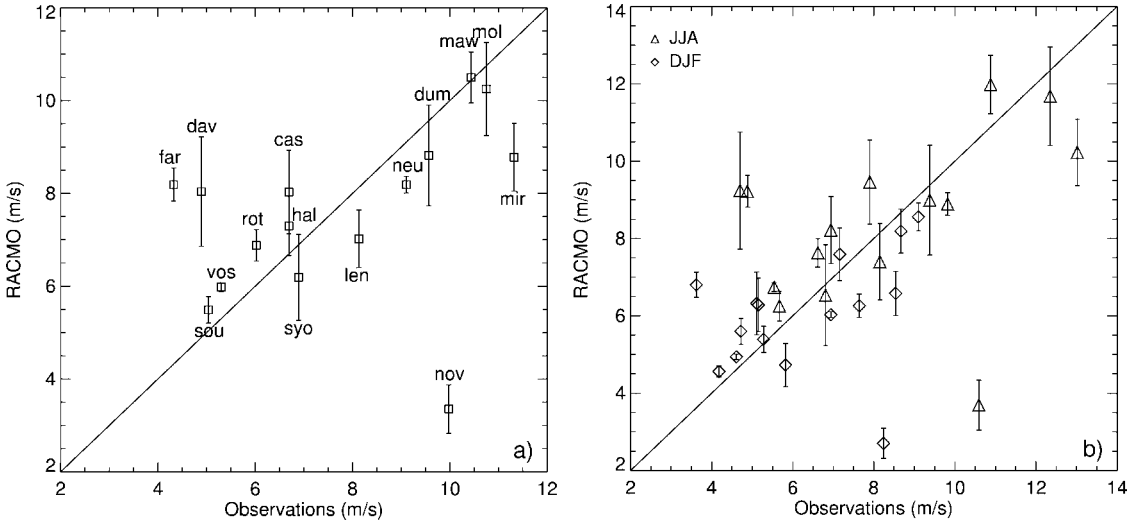

Figure 6. (a) Observed versus modelled 14 year mean 10 m wind speed for 1980–93, for 15 stations shown in Figure 1. The bars refer to the standard deviation of the 14 year mean wind speed of the nine grid points surrounding the station. (b) Observed versus modelled 14 year mean JJA (triangles) and DJF (diamonds) 10 m wind speed for 1980–93 for the same stations

At Novolazarevskaya the modelled wind speed (3.4 m s^{-1}) is much smaller than the measured wind speed (10.0 m s^{-1}). This station is located on a nunatak at the grounding line, about 75 km from a large range with rock outcrop. In state-of-the-art atmospheric models, the effect of the drag of the sub-grid-scale orography on the large-scale flow is taken into account by a formulation using an effective roughness length (derived from the variance of the sub-grid-scale orography). For Novolazarevskaya, this roughness length is 3 m, which is the upper value used in RACMO. This formulation effectively reduces the wind speed near the surface. Therefore, evaluation of the model in this region of complex orography is difficult.

A comparison between modelled and measured winter (JJA) and summer (DJF) wind speed is shown in Figure 6(b). Both in the measurements and in the model, the summer wind speed is about 75% of the winter wind speed. At half of the stations, the amplitude of the annual cycle in the wind speed is within 20% of the

Table II. Comparison of long-term mean wind speed at a line of AWSs (Allison *et al*., 1993) with RACMO wind speed. For detailed information on the data, refer to Allison *et al*. (1993)

	Dome C	D80	D57	D47	D10
Observed	3.2	6.2	9.4	10.9	8.4
Model	4.2	6.9	9.9	10.9	7.7

measured amplitude. At the remaining stations, the model has the tendency to overestimate the annual cycle. The largest difference between model and measurements occurs at the station Davis, where the observations indicate a summer maximum in the wind speed, which is not represented by the model.

Apart from the manned stations, there are also numerous AWSs in Antarctica, sampling the Antarctic near-surface wind at 3 m height. For example, a line of AWSs is situated in Adélie Land going from the Dome C station to the coast (D10 station) (Allison *et al*., 1993). We use the wind speeds that Allison *et al*. (1993: table I) derived to evaluate the RACMO output for the Adélie Land AWSs (Table II). RACMO is capable of representing the low wind speed at Dome C, where no pronounced katabatic wind occurs since it is located on the flat of a dome (Allison *et al*., 1993). Moreover, the location of the wind maximum, some distance inland of the coast, is represented by RACMO.

In summary, no systematic bias has been found in the annual mean wind speed, but the model has a tendency to overestimate the annual cycle. The largest differences between model output and measurements are found in regions of complex orography (Novolazarevskaya and Faraday), where the station might not be representative for the region covered by the grid box.

5. CONCLUSIONS

The new wind field provides a good representation of the near-surface flow across the continent that will be of value to meteorologists, glaciologists and those working in related fields. The data agree well with the available *in situ* observations and, we believe, simulate correctly the broad-scale features of the flow. Orographically related features on scales smaller than 55 km are not represented in this model.

ACKNOWLEDGEMENTS

Part of the work has been carried out within the Scientific Committee on Antarctic Research MOSAK project (Modelling and Observational Studies of Antarctic Katabatics). The modelling work was supported by the Netherlands Earth and Life Sciences Foundation (ALW) and National Computing Facilities Foundation (NCF) from the Netherlands Organization for Scientific Research (NWO). We thank Erik van Meijgaard (KNMI), Johannes Oerlemans (IMAU) and scientists from BAS for useful contributions to this work. Phil Anderson (BAS) is thanked for calculating the stream lines and helping with the interpretations of the stream-line figures and Gareth Marshall (BAS) is thanked for retrieving the ERA-40 data.

REFERENCES

Allison I, Wendler G, Radok U. 1993. Climatology of the east Antarctic ice-sheet (100°E to 140°E) derived from automatic weather stations. *Journal of Geophysical Research* **98**(D5): 8815–8823.

Bailey DA, Lynch AH, Arbetter TE. 2004. Relationship between synoptic forcing and polynya formation in the Cosmonaut Sea: 2. Regional climate model simulations. *Journal of Geophysical Research* **109**(C04023). DOI: 10.1029/2003JC001838.

Ball FK. 1960. Winds on the ice slopes of Antarctica. In *Antarctic Meteorology*, Proceedings of the Symposium of Melbourne, Australia, 1959. Pergamon Press: London; 9–16.

Bintanja R. 2001. Modelling snowdrift sublimation and its effect on the moisture budget of the atmospheric boundary layer. *Tellus Series A: Dynamic Meteorology and Oceanography* **53**(2): 215–232.

Bromwich DH. 1989. An extraordinary katabatic wind regime at Terra Nova Bay, Antarctica. *Monthly Weather Review* **117**: 688–695.

Christensen JH, Christensen OB, Lopez P, Van Meijgaard E, Botzet M. 1996. The HIRHAM4 regional atmospheric climate model, DMI Scientific Report 96-4, Copenhagen.
D'Aguanno J. 1986. Use of AVHRR data for studying katabatic winds in Antarctica. *International Journal of Remote Sensing* **7**: 703–713.
Davies HC. 1976. A lateral boundary formulation for multi-level prediction models. *Quarterly Journal of the Royal Meteorological Society* **102**: 405–418.
Gallée H, Schayes G. 1992. Dynamical aspects of katabatic wind evolution in the Antarctic coastal zone. *Boundary-Layer Meteorology* **59**: 141–161.
Genthon C, Krinner G, Cosme E. 2002. Free and laterally nudged Antarctic climate of an atmospheric general circulation model. *Monthly Weather Review* **130**: 1601–1616.
Giovinetto MB, Bromwich DH, Wendler G. 1992. Atmospheric net transport of water vapor and latent heat across 70°S. *Journal of Geophysical Research* **97**(D1): 917–930.
Heinemann G. 1997. Idealized simulations of the Antarctic katabatic wind system with a three-dimensional mesoscale model. *Journal of Geophysical Research* **102**: 13 825–13 834.
King JC. 1989. Low-level wind profiles at an Antarctic coastal station. *Antarctic Science* **1**(2): 169–178.
Mather KB, Miller GS. 1967. Notes on topographic factors affecting the surface wind in Antarctica, with special reference to katabatic winds; and bibliography. Technical Report UAG R-189, Geophysical Institute, University of Alaska.
Parish TR, Bromwich DH. 1987. The surface windfield over the Antarctic ice sheets. *Nature* **328**: 51–54.
Parish TR, Bromwich DH. 1991. Continental-scale simulation of the Antarctic katabatic wind regime. *Journal of Climate* **4**(2): 135–146.
Parish TR, Cassano JJ. 2001. Forcing of the wintertime Antarctic boundary layer winds from the NCEP–NCAR global reanalysis. *Journal of Applied Meteorology* **40**(4): 810–821.
Parish TR, Waight KT. 1987. The forcing of Antarctic katabatic winds. *Monthly Weather Review* **115**: 2214–2226.
Pettré P, Payan C, Parish TR. 1993. Interaction of katabatic wind flow with local thermal effects in coastal region of Adélie Land, East Antarctica. *Journal of Geophysical Research* **98**(D6): 10 429–10 440.
Renfrew IA, Anderson PS. 2002. The surface climatology of an ordinary katabatic wind regime in Coats Land, Antarctica. *Tellus Series A: Dynamic Meteorology and Oceanography* **54**: 463–484.
Roeckner E, Arpe K, Bengtsson L, Christoph M, Claussen M, Dümenil L, Esch M, Giorgetta M, Schlese U, Schulzweida U. 1996. The atmospheric general circulation model ECHAM-4: model description and simulation of present-day climate. Max-Planck Institut für Meteorologie, Report No. 218.
Turner J, Colwell SR, Marshall GJ, Lachlan-Cope TA, Carleton AM, Jones PD, Lagun V, Reid PA, Iagovkina S. 2004. The SCAR READER project: toward a high-quality database of mean Antarctic meteorological observations. *Journal of Climate* **17**(14): 2890–2898.
van den Broeke MR, van Lipzig NPM. 2003. Factors controlling the near-surface wind field in Antarctica, *Monthly Weather Review* **131**: 733–743.
van den Broeke MR, van Lipzig NPM, van Meijgaard E. 2002. Momentum budget of the East Antarctic atmospheric boundary layer: results of a regional climate model. *Journal of the Atmospheric Sciences* **59**(21): 3117–3129.
van Lipzig NPM, van Meijgaard E, Oerlemans J. 1999. Evaluation of a regional atmospheric climate model using measurements of surface heat exchange processes from a site in Antarctica. *Monthly Weather Review* **127**: 1994–2001.
van Lipzig NPM, van Meijgaard E, Oerlemans J. 2002. The spatial and temporal variability of the surface mass balance in Antarctica: results from a regional climate model. *International Journal of Climatology* **22**: 1197–1217.

